

Chapter 1

Voter demographics and socio-economic factors in kinetic models for opinion formation

Bertram Düring and Oliver Wright

Voter demographics and socio-economic factors like age, sex, ethnicity, education level, income, and other measurable factors like behaviour in previous elections or referenda are of key importance in modelling opinion formation dynamics. Here, we revisit the kinetic opinion formation model from *Düring and Wright* (2022) and compare in more detail the influence of different choices of characteristic demographic factors and initial conditions. The model is based on the kinetic opinion formation model by *Toscani* (2006) and the leader-follower model of *Düring et al.* (2009) which leads to a system of Fokker-Planck-type partial differential equations. In the run-up to the 2024 general election in the United Kingdom, we consider in our numerical experiments the situation in the so-called ‘Red Wall’ in North and Midlands of England and compare our simulation results to other election forecasts.

1.1 Introduction

The importance of democratic elections for societies is undisputed, and consequently pre-election polling and forecasting election outcomes based on surveys of political opinion is receiving ever growing attention. Despite pollsters stressing uncertainties in their polls and that their surveys represent momentary snapshots of opinions, weighted averages of polls as functions of time are presented by third parties in an effort to extract ‘opinion trends’ and ‘political momentum’.

Any such efforts are plagued by relatively small sample sizes of many polls, e.g. in United Kingdom with its population size of around 69 million typical sample sizes in polls are around 1000–2000. Moreover, there are many methodological issues, e.g. the coverage bias which occurs with the shift from phone to predominantly online surveys as different groups in society may not engage in online polls in the same way.

Importantly, even if a pre-election poll correctly forecasts national level vote shares, winning the election in plurality (or first-past-the-post) electoral systems (e.g. in UK or US) depends on outcomes at sub-national level. It is difficult to forecast outcomes at sub-national level from classical pre-election polls. This led to repeated (real or perceived) failures of polling. Examples include the US presidential elections of 2000

and 2016 in which polls correctly predicting the winner of the popular vote, but not of the Electoral College, and the 2015 general elections in the United Kingdom where almost every poll predicted a hung parliament, i.e. a parliament with no clear majority, but in the elections the Conservative party won with a strong majority.

In recent years, so-called multilevel regression and post-stratification (MRP) methods [29] have emerged as a promising tool to improve outcome forecasts at sub-national level. They rely on larger sample sizes and on recording demographic and socio-economic characteristics like age, sex, ethnicity, education level, income and information on previous votes in elections or referenda, in addition to the participants' voting intentions. A regression is performed to determine how likely it is that an individual with a certain combination of demographic and socio-economic characteristics votes for a particular party. In a post-stratification step, census and other publicly available data are used to determine the composition of the voter population at sub-national level, allowing to more accurately forecast the sub-national and with it also the national election outcome.

Motivated by the success of MRP methods, we have proposed and analysed a kinetic model for opinion formation which takes into account demographic and socio-economic factors like age, sex, ethnicity, education level, income and other measurable factors in [20]. Kinetic models for opinion formation have been considered by many authors, see e.g. [1–5, 7–16, 18, 19, 21, 22, 25, 26, 28, 30, 31, 33–35, 38]. Building on mathematical approaches from kinetic theory they consider the passage from interacting many-agent systems to Boltzmann-type equations. As reminiscent of binary collisions in gas theory, one considers the process of compromise between two individuals. Similar models are used in the modelling of wealth and income distributions which show Pareto tails, cf. [17] and the references therein.

In this chapter we revisit the model from [20] and compare in more detail the influence of different choices of characteristic demographic factors and initial conditions. With an interest in the upcoming 2024 general election in the United Kingdom, we consider in our numerical experiments the situation in the so-called 'Red Wall' in North and Midlands of England and compare our simulation results to other election forecasts.

The remainder of this chapter is organised as follows. In the next section, we recall the kinetic opinion formation model from [20] which takes into account demographic and socio-economic factors in the compromise process of the kinetic opinion formation model. In the quasi-invariant opinion limit this leads to a system of Fokker–Planck-type equations. In Section 1.3, we discuss the data-driven compromise functions which are used to introduce a bias into the consensus formation dynamics, depending on voter intention data. We briefly discuss the numerical discretisation of the Fokker–Planck system in Section 1.4, before we turn to an application of the model in the upcoming 2024 UK general elections in Section 1.5. We show simulation results, discuss the choice of initial conditions and demographic factors, and compare our results to other

predicted results for the upcoming election. Since the 2024 UK general election has been called for 4 July 2024 and this work was completed before this date we do not compare our results with the recorded election results.

1.2 Kinetic opinion formation model of Düring and Wright (2022)

We recall our kinetic opinion formation model from [20] in which we propose a data-driven modification leader-follower model which takes into account voter demographics, and socio-economic and other factors. It is based on the leader-follower model of Düring *et al.* [18]. Opinion is a continuous independent variable, w , in an interval $\mathcal{I} = [-1, 1]$, the other independent variable is time $t \geq 0$. The population is split into N follower species and a leader species, denoted by $f_i(w, t)$, $i = 1, 2, \dots, N$, and $f_L(w, t)$, respectively. Each follower species is associated with one combination of n “characteristics”, $c_{i1}, c_{i2}, \dots, c_{in}$, each of which is chosen from a potential set of mutually exclusive groups. These characteristics include demographic and socio-economic factors like age, sex, ethnicity, education level, income and other measurable factors like behaviour in previous elections or referenda. The leader species is formed of strong opinion leaders, as in [18], that is assertive individuals able to influence followers but withstand being influenced themselves.

The dynamics of the microscopic many-agent system are characterised by binary interactions, similar as in [18, 33]. In the present situation there are three types of possible interactions with w_L^*, v_L^* and w_L, v_L as the post- and pre-interaction leader opinions, respectively, and w^*, v^* and w, v as the post- and pre-interaction opinions of the follower species, respectively:

(a) L and L interaction:

$$\begin{aligned} w_L^* &= w_L + \gamma_L P_{LL}(w_L, v_L)(v_L - w_L) + D_L(w_L)\eta_L, \\ v_L^* &= v_L + \gamma_L P_{LL}(v_L, w_L)(w_L - v_L) + D_L(v_L)\eta_L; \end{aligned} \quad (1.1)$$

(b) i and L interaction, $i = 1, 2, \dots, N$:

$$\begin{aligned} w^* &= w + \gamma_i P_{iL}(w, v_L)(v_L - w) + D(w)\eta_i, \\ v_L^* &= v_L; \end{aligned} \quad (1.2)$$

(c) i and j interaction, $i, j = 1, 2, \dots, N$:

$$\begin{aligned} w^* &= w + \gamma_i P_{ij}(w, v)(v - w) + D(w)\eta_i, \\ v^* &= v + \gamma_j P_{ji}(v, w)(w - v) + D(v)\eta_j. \end{aligned} \quad (1.3)$$

In the interactions above, $\gamma_\nu \in (0, 1/2)$, for $\nu = 1, 2, \dots, N, L$, denotes compromise parameters which govern the “speed” of attraction of two different opinions, the functions $P_{ij}(\cdot, \cdot)$ and $D(\cdot)$ model the local relevance of compromise and self-thinking for

a given opinion, respectively, and η_ν are the “self-thinking” random variables, which model how the opinion of an individual changes independently from other individuals.

To ensure that w^* and v^* remain in \mathcal{I} , the functions P_{ij} and D, D_L functions have to be chosen accordingly, see [20]. The important novelty of this model from [20] is the introduction of data-driven functions P_{ij} which are based on polling data, explained in more detail in Section 1.3 below. A usual choice for D which we adopt also here is $D(x) = (1 - x^2)^\alpha$, for some $\alpha > 0$. We choose D_L similarly and for both $\alpha = 2$, unless otherwise stated.

Finally, we now discuss the random variables η_ν . Let us define a set of probability measures in the following way, for some $\delta > 0$:

$$\mathcal{M}_{2+\delta} = \left\{ \mathbb{P} : \mathbb{P} \text{ is a probability measure and,} \right. \\ \left. \langle |\eta|^\alpha \rangle = \int_{\mathcal{I}} |\eta|^\alpha d\mathbb{P}(\eta) < \infty, \forall \alpha \leq 2 + \delta \right\}.$$

We choose a probability density $\Theta \in \mathcal{M}_{2+\delta}$ and we assume that this density is obtained from a random variable Y with the properties, $\langle Y \rangle = \int_{\mathcal{I}} Y d\Theta(Y) = 0$, $\langle Y^2 \rangle = \int_{\mathcal{I}} Y^2 d\Theta(Y) = 1$, then we choose η_ν with the property that $\langle |\eta_\nu|^p \rangle = \langle |Y\sigma_\nu|^p \rangle$ for all $\nu = 1, 2, \dots, N, L$ and $p \in [0, 2 + \delta]$, with $0 < \sigma_\nu \ll 1$.

In the quasi-invariant limit [18, 33] $\gamma_i, \sigma_i \rightarrow 0$ with $\sigma_i^2/\gamma_i = \lambda_i$ fixed, we obtain the following Fokker-Planck-type system [20],

$$\begin{aligned} \frac{\partial}{\partial t}(f_i(w, t)) &= \frac{\partial}{\partial w} \left[\left(\frac{1}{2\tau_{iL}} \mathcal{K}_{iL}[f_L](w, t) + \sum_{j=1}^N \frac{1}{2\tau_{ij}} \mathcal{K}_{ij}[f_j](w, t) \right) f_i(w, t) \right] \\ &+ \sum_{j=1}^N \frac{\alpha_{ij}}{2\tau_{ij}} \frac{\partial}{\partial w} \left(\mathcal{K}_{ij}[f_i](w, t) f_j(w, t) \right) \\ &+ \left(\frac{\lambda_i M[f_L](t)}{4\tau_{iL}} + \sum_{j=1}^N \frac{\lambda_i M[f_j](t)}{4\tau_{ij}} \right) \frac{\partial^2}{\partial w^2} \left(D^2(w) f_i(w, t) \right) \\ &+ \sum_{j=1}^N \frac{\beta_{ij} \lambda_i M[f_i](t)}{4\tau_{ij}} \frac{\partial^2}{\partial w^2} \left(D^2(w) f_j(w, t) \right), \text{ for } i = 1, 2, \dots, N, \\ \frac{\partial}{\partial s}(f_L(w, t)) &= \frac{\alpha_{iL}}{\tau_L} \frac{\partial}{\partial w} \left(\mathcal{K}_{LL}[f_L](w, t) f_L(w, t) \right) \\ &+ \frac{\beta_{iL} \lambda_L M[f_L](t)}{2\tau_L} \frac{\partial^2}{\partial w^2} \left(D_L^2(w) f_L(w, t) \right), \end{aligned} \quad (1.4)$$

where, with $\xi, \mu, \nu = 1, 2, \dots, N, L$,

$$\mathcal{K}_{\mu\nu}[f_\xi](w, t) := \int_{\mathcal{I}} P_{\mu\nu}(w, v)(v - w) f_\xi(v, t) dv, \quad M[f_\xi](t) := \int_{\mathcal{I}} f_\xi(w, t) dw.$$

1.3 Compromise function from demographic voter intention data

In [20] a data-driven approach to include demographic and other factors into the compromise function has been introduced whereas previously, the compromise function P has been chosen as a localisation function, see e.g. [18, 19, 33]. To this end, data from voter intention polls made before the election are employed.

Let there be political parties, $\Pi_1, \dots, \Pi_{\mathcal{P}}$, and $p_0 < p_1 < \dots < p_{\mathcal{P}-1} < p_{\mathcal{P}}$ be a partition of \mathcal{I} , then we associate the mass of the leader species in an influence interval $\mathcal{I}_{\zeta} = [p_{\zeta-1}, p_{\zeta}]$ with a political party standing in the election. The fractional masses of follower species contained within an influence interval are assumed to vote for the controlling party, and give rise to influence masses,

$$M_{\zeta,i}(t) = \int_{\mathcal{I}_{\zeta}} f_i(w, t) dw$$

for every $\zeta = 1, \dots, \mathcal{P}$. Figure 1.1 shows a schematic representation.

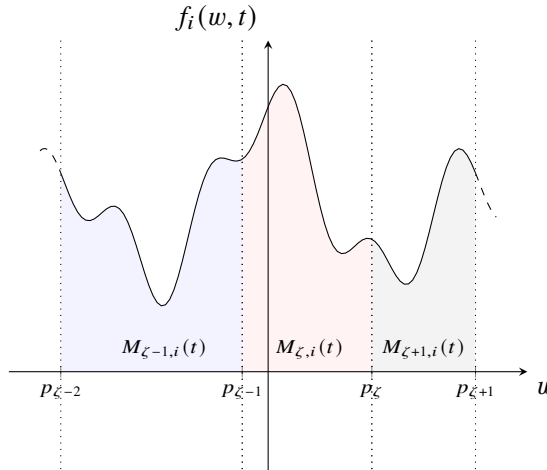


Figure 1.1. Schematic representation of influence masses for a given density function, $f_i(w, t)$, at some time t .

Typical voter intention data is organised in tables by characteristics, with parties on the vertical axis and the groups (e.g. leave and remain for 2016 Brexit Vote, 18-24 year-old etc. for age) on the horizontal axis. A table for an example characteristic k is displayed in Table 1.1 and the actual table from [37] for 2024 voter intention data relating to their 2016 Brexit referendum vote is displayed in Table 1.2.

For each binary interaction (1.1)–(1.3) we can find the influence intervals \mathcal{I}_{ζ} to which w, v belong to, assume that $w \in \mathcal{I}_{\mu}$ and $v \in \mathcal{I}_{\nu}$, for some $\mu, \nu = 1, \dots, \mathcal{P}$. We look up the relevant values in the tables to get the values of $x_{\mu,i,k}$ and $x_{\nu,j,k}$.

Table 1.1. Example of how the characteristic data is presented.

Characteristic k	Group 1	Group 2	\cdots	Group m
Π_1	$x_{1,1,k}$	$x_{1,2,k}$	\cdots	$x_{1,m,k}$
Π_2	$x_{2,1,k}$	$x_{2,2,k}$	\cdots	$x_{2,m,k}$
\vdots	\vdots	\vdots	\ddots	\vdots
$\Pi_{\mathcal{P}}$	$x_{\mathcal{P},1,k}$	$x_{\mathcal{P},2,k}$	\cdots	$x_{\mathcal{P},m,k}$

Table 1.2. The 2024 voter intention data relating to their 2016 Brexit referendum vote from [37].

Brexit Vote	Leave	Remain
Labour	0.17	0.51
Green	0.03	0.08
LibDems	0.07	0.19
Other	0.05	0.08
Conservative	0.35	0.11
Brexit	0.33	0.03

Let w, v be the opinions of two individuals in follower species i and j , respectively, with associated characteristic groups c_{ik}, c_{jk} for all $k = 1, \dots, n$, we use the following compromise function decomposition:

$$P_{ij}(w, v) = P_{loc}(w, v) \prod_{k=1}^n P_{char}(w, v, c_{i,k}, c_{j,k}). \quad (1.5)$$

We consider the localisation function,

$$P_{loc}(w, v) = \mathbf{1}_{[-r,r]}(w - v),$$

for some $r > 0$ where $\mathbf{1}_A(x)$ denotes the characteristic function for the set A .

For the leader species interactions $P_{iL}(w, v) = P_{LL}(w, v) = P_{loc}(w, v)$. For follower species interactions, we use the characteristic comparison function

$$P_{char}(w, v, c_{i,k}, c_{j,k}) = \sum_{\mu, \nu=1}^{\mathcal{P}} \mathbf{1}_{[p_{\mu-1}, p_{\mu}]}(w) \mathbf{1}_{[p_{\nu-1}, p_{\nu}]}(v) F(x_{\mu,i,k} - x_{\nu,j,k}), \quad (1.6)$$

with

$$F(x) = \left(1 - \left(\frac{1}{4}(2+x) \right)^a \right)^b,$$

and $a, b > 0$ as in [20]. The characteristic comparison function P_{char} models the idea of net movement towards more popular opinions, as indicated by voter intention data from pre-election polls. Individuals with current popular opinions move slower towards unpopular opinions than individuals with current unpopular opinions move towards more popular opinions. The argument of the function, $x_{\mu,i,k} - x_{\nu,j,k}$, gives a large, positive value when the party, in whose influence the individual resides, is more popular (i.e $x_{\mu,i,k}$ dominates) and a large negative value when the party, in whose influence the other individual resides, is more popular (i.e $x_{\nu,j,k}$ dominates). When both parties are equally popular, this value will be zero and therefore will not have a bias towards one party or the other. Therefore, the difference $x_{\mu,i,k} - x_{\nu,j,k}$ is representative of the popularity of individuals' opinion.

1.4 Numerical experiments

For purposes of the discretisation of the Fokker-Plank system (1.4) we employ a finite element method. Let (f, g) denote the L^2 inner product of the function f and g , $(f, g) = \int_{\mathcal{I}} f(w) \cdot g(w) dw$. We have chosen the values of $a = 2$ and $b = 8$ in the P_{char} function since these have offered the best results, $\alpha_i = \beta_i = 1$ for all $i = 1, 2, \dots, N, L$. We construct our initial densities from available polling data and from population values for the specific region we wish to run simulations in. We do this by first finding the influence mass of the Party Π_ζ for a given species i , multiplying the relevant columns of our data tables, which, for a species whose members have characteristic k and are in Group ξ , is the ξ -th column from Table 1.1 and the relevant column from every characteristics table, element-wise. We will call the elements of the resulting column $X_{\zeta,i}$. Recall that by definition

$$M_i = \sum_{\zeta} M_{\zeta,i},$$

where we recall that $M_{\zeta,i}$ are the influence masses from Section 1.3. Given some distribution of mass between the follower species M_i , we can compute the initial influence masses for the parties in

$$M_{\zeta,i} = \frac{v_{\zeta} X_{\zeta,i}}{\sum_{\zeta} v_{\zeta} X_{\zeta,i}} M_i,$$

with v_{ζ} being the percentage of votes allocated to Π_{ζ} in some test election, either through the recorded results of some previous election or some pre-election polling data. We define the initial densities of the species as a weighted sum of characteristic functions in the following way

$$f_i(w, 0) = \sum_{\zeta} M_{\zeta,i} \mathbb{1}_{w \in \mathcal{I}_{\zeta}},$$

for all $\zeta = 1, 2, \dots, N$.

The initial density of the leader species is chosen as a weighted sum of delta distributions,

$$f_L(w, 0) = \sum_{k=1}^6 p_k \delta(w - L_k), \quad (1.7)$$

with p_k representing the percentage of the vote that each party attained in this, or another, test election, and L_k representing the party locations. In all the simulations presented here, we set the mass of the leader species to have 5% the total mass of the follower species, in a similar way to *Düring et al* [18].

We approximated the delta functions in $f_L(w, 0)$ with the scaled mollifier functions

$$\phi(x) = \begin{cases} \exp\left(-\frac{(x/\varepsilon)^2}{1 - (x/\varepsilon)^2}\right), & \text{for } x \in [-1, 1], \\ 0, & \text{otherwise,} \end{cases}$$

with scale factor $\varepsilon \ll 1$.

We discretise our time axis with $A = 300$ nodal points, and space axis with $B = 100$ nodal points. We write the nodal values of our functions $f_i(w_k, t^n) = f_{i,k}^n$ and the vector of every spatial nodal value, at time $t^n > 0$, as \mathbf{f}_i^n . We then use a semi-implicit Euler method to discretise our coupled system of non-linear, non-local PDEs in time and an FEM for discretisation in space, with quadratic, Lagrangian basis functions $b_k \in C_c(\mathcal{I}; \mathbb{R})$ for $k = 1, 2, \dots, B$, which leads to the following linear system:

$$\sum_{i=1}^N \left((\mathbf{M} + \mathbf{U}_i - \mathbf{C}_{Li}^n) \mathbf{f}_i^{n+1} + \sum_{j=1}^N (\mathbf{V}_{ij} - \mathbf{T}_{ij}^n) \mathbf{f}_j^{n+1} \right) = \sum_{i=1}^N \mathbf{M} \mathbf{f}_i^n, \quad (1.8)$$

where $\mathbf{M} = (b_k, b_l)_{(k,l)}$ is the mass matrix, \mathbf{C}_{Li}^n and \mathbf{T}_{ij}^n are the discretised transport matrices, given by

$$\mathbf{C}_{Li}^n = \Delta t \left(\left[\frac{1}{2\tau_{iL}} K_{L,iL}^n + \sum_{j=1}^N \frac{1}{2\tau_{ij}} K_{j,ij}^n \right] b_k, b'_l \right)_{(k,l)},$$

$$\mathbf{T}_{ij}^n = \Delta t \left(\frac{\alpha_{ij}}{2\tau_{ij}} K_{i,ij}^n b_k, b'_l \right)_{(k,l)},$$

with $K_{L,iL}^n(w)$ and $K_{m,ij}^n(w)$ as the midpoint rule approximation of the convolution operators, $\mathcal{K}_{ij}[f_m](w, t^n)$ evaluated at the previous time step, in the transport terms of the Fokker-Planck equations and \mathbf{U}_i and \mathbf{V}_{ij} are the discretised Laplacian term

matrices,

$$\mathbf{U}_i = \Delta t \left(\left[\frac{\lambda_i M_L}{4\tau_{iL}} + \sum_{j=1}^N \frac{\lambda_i M_j}{4\tau_{ij}} \right] D^2 b'_k, b'_l \right)_{(k,l)},$$

$$\mathbf{V}_{ij} = \Delta t \left(\frac{\lambda_i M_j \beta_{ij}^2}{4\tau_{ij} \alpha_{ij}} D^2 b'_k, b'_l \right)_{(k,l)}.$$

1.5 Application to the 2024 General Election in the United Kingdom

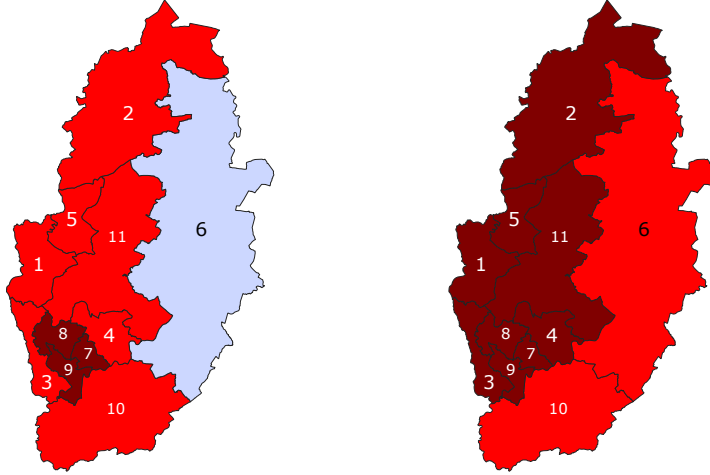
In this section, we consider the upcoming 2024 general election in the United Kingdom, focusing on Nottinghamshire as part of the so-called Red Wall (a group of constituencies in the North and Midlands of the UK traditionally dominated by Labour), as in [20]. When comparing with the earlier results, note that in the time between this work and the one presented in [20], the Brexit party has been renamed to Reform UK and we will use this name throughout this work. Also the constituency boundaries have been modified and subsequently the constituencies of Nottingham North and Sherwood have been renamed to Nottingham North and Kimberley and Sherwood Forest, respectively.

We present here a blanket of possible results that could arise from these models. Namely, we will consider the use of different demographics when defining the follower species, the use of universal initial conditions and investigate the role of the maximum time used in the model. Finally, we compare the results from these investigations with other predictions of the election.

Unless otherwise stated, we again use the parameters $\tau_{iL} = 0.05$, $\tau_{ij} = 2.5$, $\lambda = 0.033$, $\Delta t = 0.1$ and $r = 0.85$. Initial masses and regionalised data are produced similarly to [20] with the exception that we use a more recent poll from YouGov as our voting intention data [37]. Other data used are 2011 Census data [27], results of the 2017, 2019 UK general elections [23,24], and results of the 2016 EU referendum [32].

1.5.1 Investigating the number of time steps

In this experiment, we explore the effect of changing the final time of the model. In previous examples, we have left the model to run for very large times, in order to reach the equilibrium state. However this may not be a particularly realistic method, and may lead to over-fitting the model to the original data. Therefore in this experiment, we run the model for both $A = 10$ and $A = 100$ to investigate this difference. Note that although the time steps are different in each model, the change in time between time steps Δt remains at 0.1 – that is the final time will be 1 in the first model and 10 in the second.



(a) Predicted Result from the kinetic model with $A = 10$. (b) Predicted Result from the kinetic model with $A = 100$.

Figure 1.2. Predicted Results of the General Elections in 2024 in Nottinghamshire with different total timesteps. Light colours (Labour in red, Conservative in blue) are where the total popular vote for the elected MP was below 50% and the dark colours for greater than 50%.

The results are presented in Figure 1.2, with colour-coding of each constituency, red if a Labour MP was elected, blue if a Conservative MP was elected. The light colours are where the total popular vote for the elected MP was below 50% and the dark colours for greater than 50%. The results show a stark difference in final winning percentage, but not the winning party in all constituencies, except (6) Newark, however the final results in the model Figure 1.2a, the difference between Labour and Conservative are very small compared to the other constituencies. It would appear that using a much higher final time for the model does lead to some over-fitting but the strength of this effect and the optimal stopping time are left as areas of further study. In the following models, we take the number of temporal nodal points to be $A = 10$.

1.5.2 Investigating the choice of initial condition

We discuss here the idea of using universal initial conditions against the demographic specific version used in [20] (demographic initial conditions) in the Fokker-Planck model. Our universal initial conditions are defined using the raw previous election data for that constituency, that is when discussing $M_{\zeta,i}$ we use directly the value of v_{ζ} leaving us with the definition of $M_{\zeta,i}$ as,

$$M_{\zeta,i} = \frac{v_{\zeta}}{\sum_{\zeta} v_{\zeta}} M_i,$$

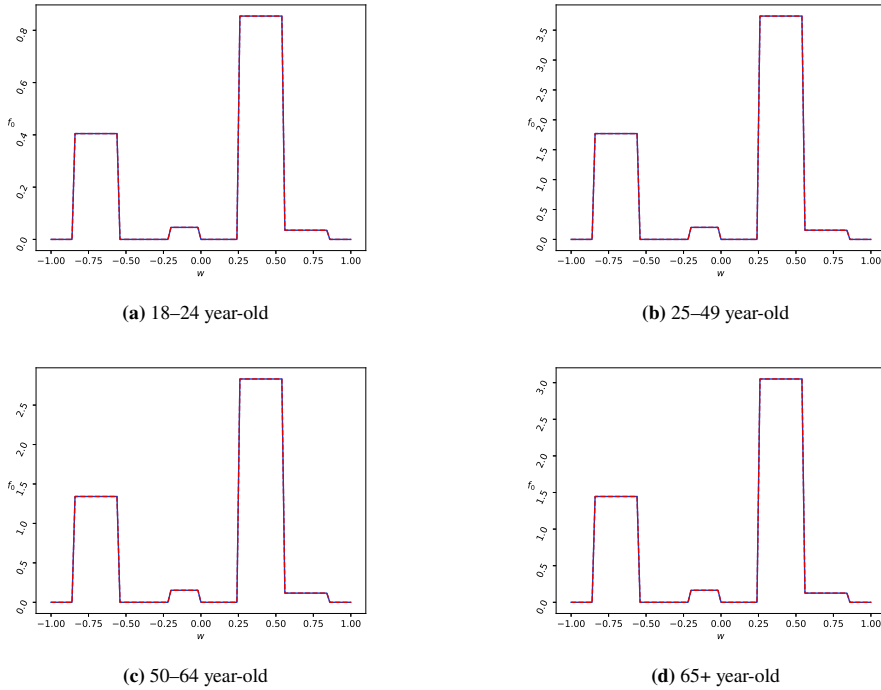


Figure 1.3. Universal initial densities for the eight follower species in the constituency of Newark from the 2017 General Election Results. Each graph shows the initial density for the leave (dashed red) and the remain (solid blue) characteristic of an age group.

with v_ζ representing the percentage of votes allocated to a given party, Π_ζ , is some test election in each individual constituency. In this case we have chosen our test election to be the UK general election in 2017. This method makes the assumption that the vote from the 2017 general election was consistent across demographic. We believe this assumption is reasonable since the population age demographic of an individual in 2017 may be different from the age demographic in 2024 – that is an individual who was 19 years old in 2017 will be 26 in 2024 and their views on political subjects may or may not have changed accordingly. In the previous work [20], we had assumed that through a reasonable usage of data, a more specific initial condition based on demographic could be synthesised. It is crucial to note at this point that in the absence of local polling data from the areas, an initial condition for this model is necessarily inaccurate. A graphical representation of the proposed universal initial conditions and the demographic initial conditions used in [20] for the constituency of (6) Newark are presented in Figure 1.3 and Figure 1.4, respectively.

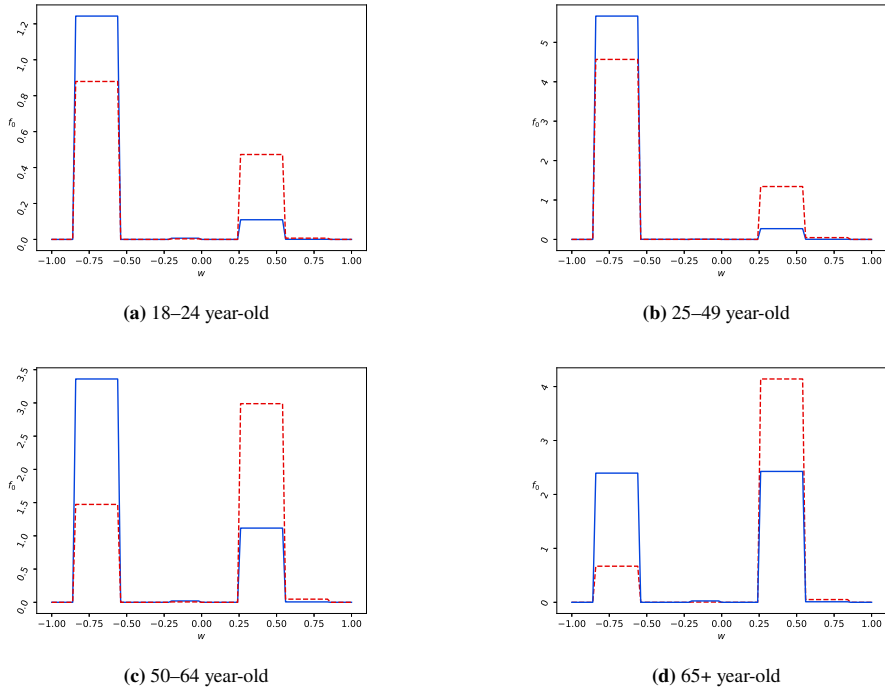
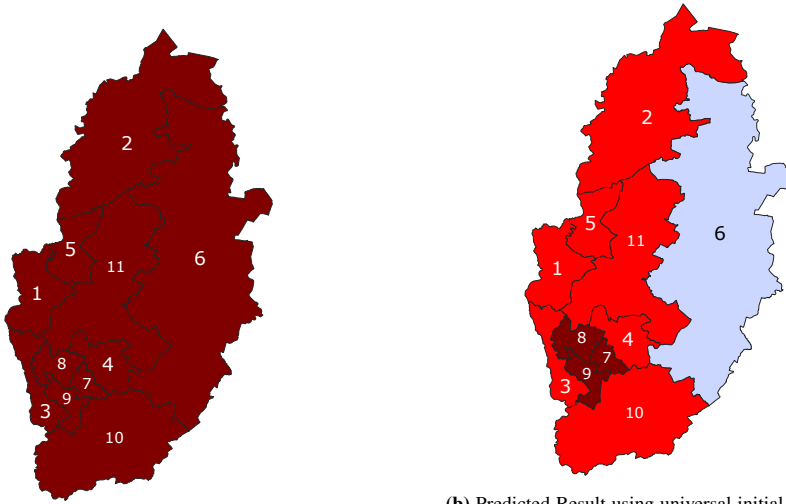


Figure 1.4. Demographically motivated initial densities for the eight follower species in the constituency of Newark from the 2017 General Election Results. Each graph shows the initial density for the leave (dashed red) and the remain (solid blue) characteristic of an age group.

The results are presented in Figure 1.5 with colour-coding of each constituency, red if a Labour MP was elected, blue if a Conservative MP was elected. The light colours are where the total popular vote for the elected MP was below 50% and the dark colours for greater than 50%. We can see that using the demographic initial conditions result in more extreme results – every constituency in Nottingham is predicted a greater than 50% vote share for Labour – and the universal initial conditions have less extreme result – only (7) Nottingham East, (9) South and (8) Nottingham North and Kimberley are predicted a greater than 50% vote share for Labour. (6) Newark is of particular interest in this case because it is predicted to vote overwhelmingly Labour in Figure 1.5a and slightly Conservative in Figure 1.5b. The final weighted sum of vote shares from the demographics is presented in Table 1.3.

This effect across all constituencies is likely due to the way the demographic initial conditions incorporate the voter intention data. In order to distinguish the initial conditions in [20], voter intention data was multiplied together element by element and then combined with the 2015 election result. However this “double” usage of the voter



(a) Predicted Result using initial conditions as in [20].

(b) Predicted Result using universal initial conditions from GE2017 results.

Figure 1.5. Comparison between the different choices of initial conditions. Light colours (Labour in red, Conservative in blue) are where the total popular vote for the elected MP was below 50% and the dark colours for greater than 50%.

Table 1.3. The weighted sum of the predicted vote shares from the demographics in the demographic initial conditions and universal initial conditions.

Newark	Lab	Grn	LibD	Oth	Con	RefUK
Demographic IC	52.5%	7.24%	3.02%	6.00%	17.7%	13.6%
Universal IC	27.7%	5.65%	4.35%	9.84%	29.8%	22.6%

intention data – once in the initial conditions, once in the choice of P – makes the kinetic model susceptible to extremities in voter intention data. In the 2024 election, it has been predicted many times that Labour will win [37] and this is reflected in the voter intention data, however this likely leads to a situation with the simple demographic initial conditions, that we see above.

In subsequent experiments we will use the universal initial conditions, since this allows for a comparison of the final results without bias from the initial conditions.

1.5.3 Investigating the choice of demographics

In previous examples we have constructed our follower species from two demographics – namely age demographic (18-24yo, 25-49yo, 50-64yo and 65+yo) and self reported Brexit vote (leave, remain). In this experiment, we compare the contribution to pre-

dicted results from using these original follower species and eight follower species using NRS social grade (ABC1, C2DE) to replace Brexit vote. The Brexit vote had an impact on the previous election [6], and may have an impact on the current election, however choosing to use social grade is due to its historic effect on voting in UK general elections.

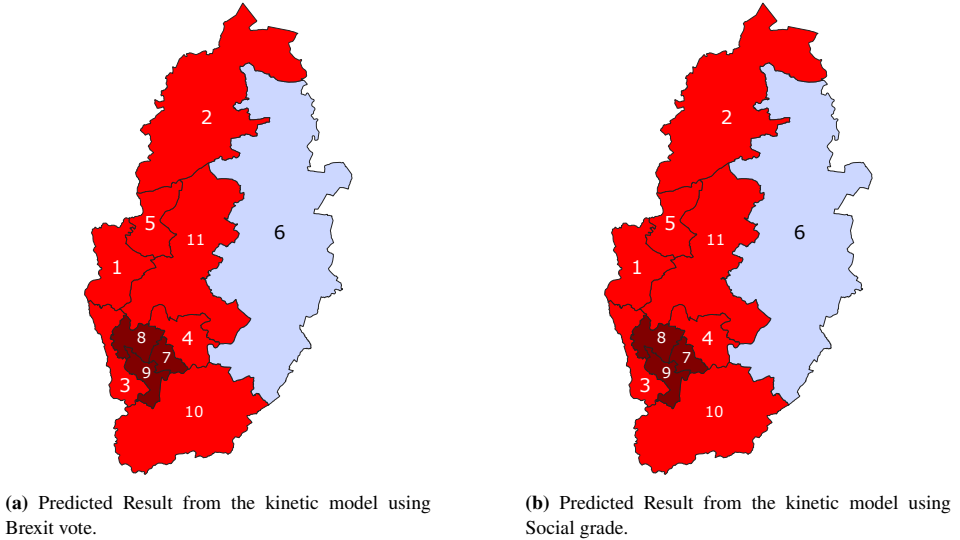


Figure 1.6. Predicted Results of the General Elections in 2024 in Nottinghamshire according to the model presented here, (1.6a) using Brexit vote and age and, (1.6b) using social grade and age. The light colours (Labour in red, Conservative in blue) are where the total popular vote for the elected MP was below 50% and the dark colours for greater than 50%.

From the results presented in Figure 1.6, we can see that the party that is predicted a majority by the model does not change when changing the demographic composition of the follower species. We cannot determine whether this result will be true for all elections, since some particular choice of demographic may have some political significance – as the Brexit vote did in [20] – however it appears as though these effects are less extreme in this election. Since both of these models agree in this case, we will continue to use the Brexit vote as the indicator for this election.

1.5.4 Comparison to other predicted results

Since the 2024 UK general election has been called for 4th July and this work was completed before this date, we cannot compare the model results directly to the recorded results, however we can compare to other model predictions, such as that of YouGov [36]. Both these methods utilise the MRP method for the prediction and use proper

regionalised data, whereas we are using national data, that has been regionalised using the method presented in [20].

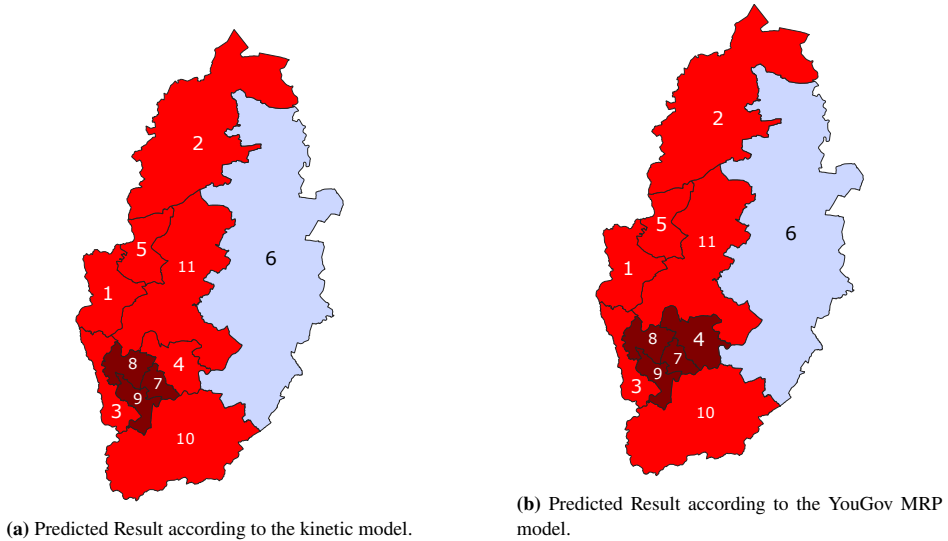


Figure 1.7. Predicted Results of the General Elections in 2024 in Nottinghamshire according to the model presented here, with $T = 10$ (1.7a) and the MRP model presented by YouGov (1.7b). The light colours (Labour in red, Conservative in blue) are where the total popular vote for the elected MP was below 50% and the dark colours for greater than 50%.

As we can see from the results in Figure 1.7, our simulation results are inline with a direct comparison with the MRP method by YouGov, with a few major differences. In terms of full results, this model predicts a less extreme win in (4) Gedling. Importantly, the secondary and tertiary results in each region, in the cases of (2) Bassetlaw, (3) Broxtowe, (4) Gedling, (5) Mansfield, (10) Rushcliffe and (11) Sherwood Forest, both the YouGov prediction and the result from the kinetic model rank at least the first three parties the same – for all of these the ranks are 1) Labour, 2) Conservative and 3) Reform UK – in (1) Ashfield, the Reform UK candidate, Lee Anderson, has recently defected from the Conservative party to Reform UK and is the incumbent MP in that region. We believe that for at least this case, more localised data would have been more indicative of the situation, however since we have used national data and regionalised this to a smaller area, we necessarily miss local opinions on MPs. We wish to reiterate, however, that these models agree with YouGov on which MP will have the number one ranking in each constituency, and in FPTP elections, this is the determining statistic that informs which party will win the seat. This again demonstrates the potential use of these models for election prediction.

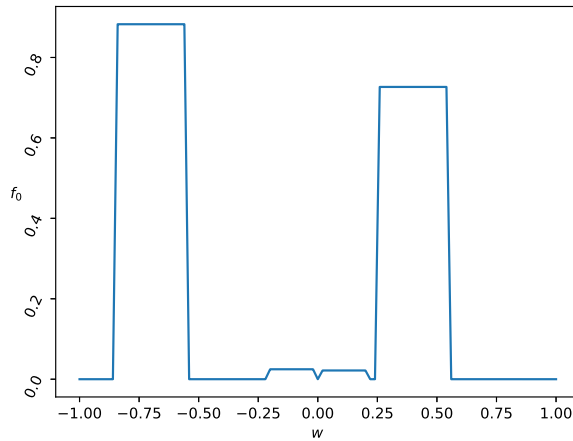


Figure 1.8. The initial density for all eight follower species in Bassetlaw for the 2024 general election.

1.5.5 A more in depth look at Bassetlaw

We take a closer look at the constituency of Bassetlaw. We believe this constituency is of particular interest since, the seat of Bassetlaw had elected the candidate from the Labour party since 1929 with the only break being in 1931-35, where the National Labour Group – split from the Labour party – were incumbent. In 2019, Bassetlaw elected the candidate from the Conservative Party, Brendan Clarke-Smith, and from both the model presented here and the model presented by YouGov, the Labour Candidate is predicted to win this seat again.

The eight initial follower densities presented in Figure 1.8 using universal initial conditions, from the 2017 General Election.

As we can see from Figure 1.9, the final time graphs are very similar for all eight follower species. The 18-24yo species have slightly more mass in the Labour influence than the 65+yo and there is a very slight separation between leave (red dotted) and remain (solid blue). In this election, YouGov and Election Calculus both predict a strong majority for Labour over the Conservatives, and this is especially strong in the Red Wall. These graphs will be different if we were to use true local polling data, however the collated result in Bassetlaw is very similar to that of YouGov and Electoral Calculus.

We also wish to compare the results in Figure 1.9, to the results obtained using $A = 100$, Figure 1.10, since this clearly shows a lack of differentiation between the

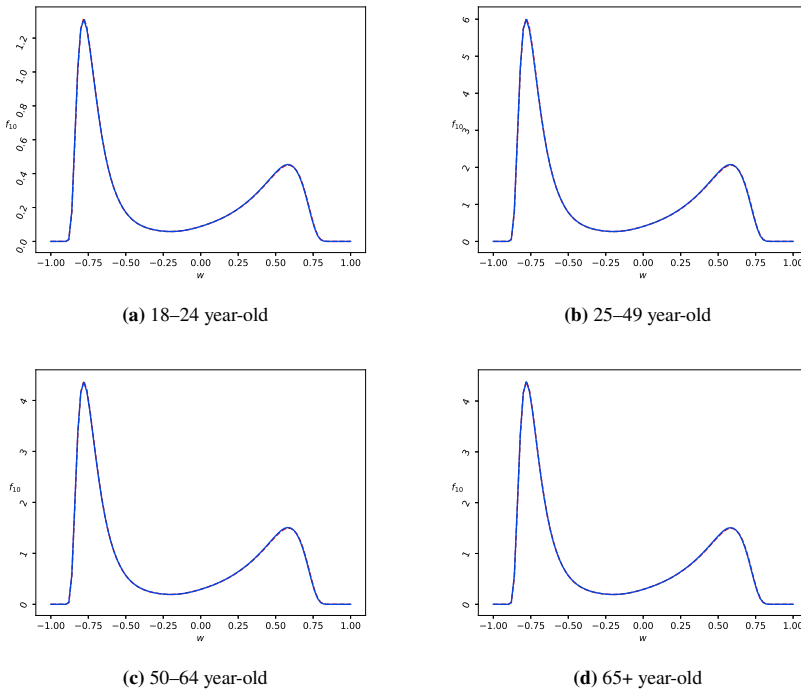


Figure 1.9. Final time graphical representations of the predicted result from our kinetic model with $A = 10$ in Bassetlaw in the 2024 General Election.

follower species in Bassetlaw, even when looking at substantially longer time steps. This confirms that our prediction is we should see a strong Labour win in Bassetlaw.

Funding. This work was partially supported by a Royal Society International Exchanges grant (Ref. IES/R3/213113). O.W. is supported by the Warwick Mathematics Institute Centre for Doctoral Training in Mathematics, and gratefully acknowledges funding from the University of Warwick.

References

[1] G. Albi, E. Calzola, and G. Dimarco, [A data-driven kinetic model for opinion dynamics with social network contacts](#). *European Journal of Applied Mathematics* (2024), 1–27

[2] G. Albi, L. Pareschi, G. Toscani, and M. Zanella, [Recent advances in opinion modeling: control and social influence](#). In *Active Particles, Volume 1. Modeling and Simulation in Science, Engineering and Technology*, edited by N. Bellomo, P. Degond, and E. Tadmor, pp. 49–98, Birkhäuser, Cham, 2017

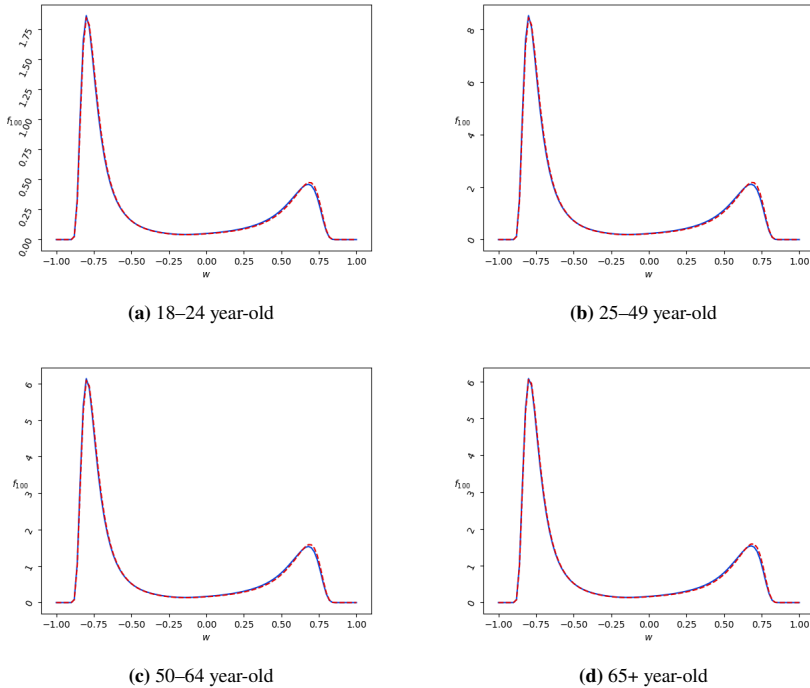


Figure 1.10. Final time graphical representations of the predicted result from our kinetic model with $A = 100$ in Bassetlaw in the 2024 General Election.

- [3] G. Albi, L. Pareschi, and M. Zanella, [On the optimal control of opinion dynamics on evolving networks](#). In *System modeling and optimization*, edited by L. Bociu, J.-A. Désidéri, and A. Habbal, pp. 58–67, Springer, Cham, 2016
- [4] G. Albi, L. Pareschi, and M. Zanella, [Opinion dynamics over complex networks: kinetic modeling and numerical methods](#). *Kinet. Relat. Models* **10** (2017), 1–32
- [5] G. Albi, L. Pareschi, and M. Zanella, [Boltzmann games in heterogeneous consensus dynamics](#). *J. Stat. Phys.* **175** (2019), no. 1, 97–125
- [6] BBC News, General election 2019: Conservatives take Wakefield from Labour. 2019, URL <https://www.bbc.co.uk/news/election-2019-50772224>, last accessed 1 July 2021
- [7] N. Bellomo, F. Colasuonno, D. Knopoff, and J. Soler, [From a systems theory of sociology to modeling the onset and evolution of criminality](#). *Netw. Heterog. Media* **10** (2015), no. 3, 421–441
- [8] M. L. Bertotti and M. Delitala, [On a discrete generalized kinetic approach for modelling persuader’s influence in opinion formation processes](#). *Math. comput. model.* **48** (2008), no. 7–8, 1107–1121

- [9] L. Boudin and F. Salvarani, [Opinion dynamics: kinetic modelling with mass media, application to the Scottish independence referendum](#). *Physica A* **444** (2016), 448–457
- [10] M. Burger, [Network structured kinetic models of social interactions](#). *Vietnam J. Math.* (2021)
- [11] M. Burger, M. Di Francesco, S. Fagioli, and A. Stevens, [Sorting phenomena in a mathematical model for two mutually attracting/repelling species](#). *SIAM J. Math. Anal.* **50** (2018), no. 3, 3210–3250
- [12] B. Chazelle, Q. Jiu, Q. Li, and C. Wang, [Well-posedness of the limiting equation of a noisy consensus model in opinion dynamics](#). *J. Differ. Equations* **263** (2017), no. 1, 365–397
- [13] E. Cristiani and A. Tosin, [Reducing complexity of multiagent systems with symmetry breaking: an application to opinion dynamics with polls](#). *Multiscale Model. Simul.* **16** (2018), no. 1, 528–549
- [14] P. Degond, J.-G. Liu, S. Merino-Aceituno, and T. Tardiveau, [Continuum dynamics of the intention field under weakly cohesive social interaction](#). *Math. Models Methods Appl. Sci.* **27** (2017), no. 1, 159–182
- [15] B. Düring, J. Franceschi, M.-T. Wolfram, and M. Zanella, [Breaking consensus in kinetic opinion formation models on graphons](#). *Journal of Nonlinear Science* **34** (2024), no. 4, 79
- [16] B. Düring, A. Jüngel, and L. Trussardi, [A kinetic equation for economic value estimation with irrationality and herding](#). *Kinet. Relat. Models* **10** (2017), no. 1, 239–261
- [17] B. Düring, D. Matthes, and G. Toscani, [Kinetic equations modelling wealth redistribution: A comparison of approaches](#). *Phys. Rev. E* **78** (2008), 056103
- [18] B. Düring, P. Markowich, J. Pietschmann, and M. Wolfram, [Boltzmann and Fokker-Planck equations modelling opinion formation in the presence of strong leaders](#). *Proc. R. Soc. A.* **465** (2009), 3687–3708
- [19] B. Düring and M. Wolfram, [Opinion dynamics: inhomogeneous Boltzmann-type equations modelling opinion leadership and political segregation](#). *Proc. R. Soc. A.* **471** (2015), 20150345
- [20] B. Düring and O. Wright, [On a kinetic opinion formation model for pre-election polling](#). *Phil. Trans. R. Soc. A.* **380** (2022), no. 2224, 20210154
- [21] G. Furioli, A. Pulvirenti, E. Terraneo, and G. Toscani, [Fokker-Planck equations in the modeling of socio-economic phenomena](#). *Math. Models Methods Appl. Sci.* **27** (2017), no. 1, 115–158
- [22] J. Garnier, G. Papanicolaou, and T.-W. Yang, [Consensus convergence with stochastic effects](#). *Vietnam J. Math.* **45** (2017), no. 1-2, 51–75
- [23] House of Commons Library, Data file: detailed results by constituency [microsoft excel spreadsheet]. 2019, URL <https://commonslibrary.parliament.uk/research-briefings/cbp-7979>, last accessed 5 March 2021
- [24] House of Commons Library, Data file: detailed results by constituency [microsoft excel spreadsheet]. 2021, URL <https://commonslibrary.parliament.uk/research-briefings/cbp-8749>, last accessed 9 June 2021

- [25] P.-E. Jabin and S. Motsch, [Clustering and asymptotic behavior in opinion formation](#). *J. Differ. Equations* **257** (2014), no. 11, 4165–4187
- [26] S. Motsch and E. Tadmor, [Heterophilious dynamics enhances consensus](#). *SIAM Rev.* **56** (2014), no. 4, 577–621
- [27] Office of National Statistics, 2011 census, KS102EW age structure, local authorities in England and Wales. 2012, URL <http://www.nomisweb.co.uk/census/2011/ks102ew>, last accessed 1 March 2021.
- [28] L. Pareschi, G. Toscani, A. Tosin, and M. Zanella, [Hydrodynamic models of preference formation in multi-agent societies](#). *J. Nonlinear Sci.* **29** (2019), no. 6, 2761–2796
- [29] D. K. Park, A. Gelman, and J. Bafumi, [Bayesian multilevel estimation with poststratification: State-level estimates from national polls](#). *Political Anal.* **12** (2004), 375–385
- [30] L. Pedraza, J. P. Pinasco, and N. Saintier, [Measure-valued opinion dynamics](#). *Math. Models Methods Appl. Sci.* **30** (2020), no. 2, 225–260
- [31] M. Pérez-Llanos, J. P. Pinasco, N. Saintier, and A. Silva, [Opinion formation models with heterogeneous persuasion and zealotry](#). *SIAM J. Math. Anal.* **50** (2018), no. 5, 4812–4837
- [32] The Electoral Commission, Results and turnout at the EU referendum. 2019, URL <https://www.electoralcommission.org.uk/who-we-are-and-what-we-do/elections-and-referendums/past-elections-and-referendums/eu-referendum/results-and-turnout-eu-referendum>, last accessed 16 April 2021
- [33] G. Toscani, [Kinetic models of opinion formation](#). *Comm. Math. Sci.* **4** (2006), no. 3, 481–496
- [34] G. Toscani and L. Pareschi, *Interacting Multiagent Systems*. Oxford University Press, 2013
- [35] G. Toscani, A. Tosin, and M. Zanella, [Opinion modeling on social media and marketing aspects](#). *Phys. Rev. E* **98** (2018), no. 2, 022315
- [36] YouGov, UK general election 2024. 2024, URL <https://yougov.co.uk/elections/uk/2024>, last accessed 29 June 2024
- [37] YouGov, Voting intention. 2024, URL <https://yougov.co.uk/topics/politics/trackers/voting-intention>, last accessed 29 June 2024
- [38] M. Zanella, [Kinetic models for epidemic dynamics in the presence of opinion polarization](#). *Bulletin of Mathematical Biology* **85** (2023), no. 5, 36